Electronic Supplementary Material (ESI) for Journal of Materials Chemistry B.

Supplementary information

Tumor-Targeting Polymer Nanohybrids with Amplified ROS Generation for Photodynamic-Combination Chemodynamic Therapy

Xiaodan Chen,‡[a,b] Danling Cheng,‡[c] Ningyue Yu,[c] Jian Feng,[c] Jingchao Li,*[c] Lin Lin*[b]

[a] *Department of Radiology, Clinical Oncology School of Fujian Medical University, Fujian Cancer Hospital, Fuzhou 350014, China*

[b] *Department of Radiology, Fujian Medical University Union Hospital, Fuzhou 350001, China. Email: linlin@fjmu.edu.cn*

[c] *College of Biological Science and Medical Engineering, Donghua University, Shanghai 201620, China. Email: jcli@dhu.edu.cn*

‡ *Ccontributed equally to this work.*

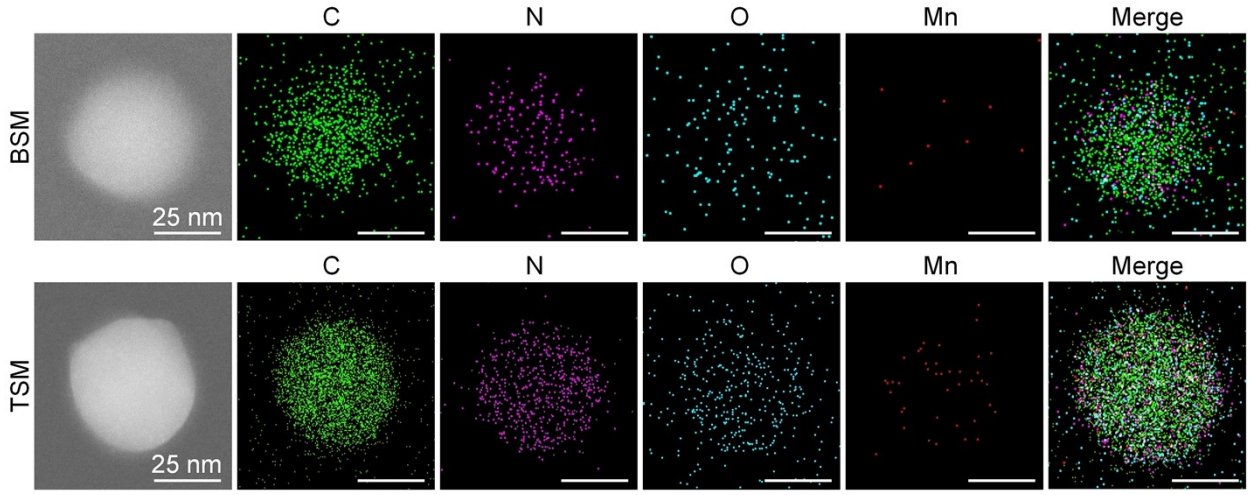

Fig. S1. Elemental mapping images of BSM and TSM.

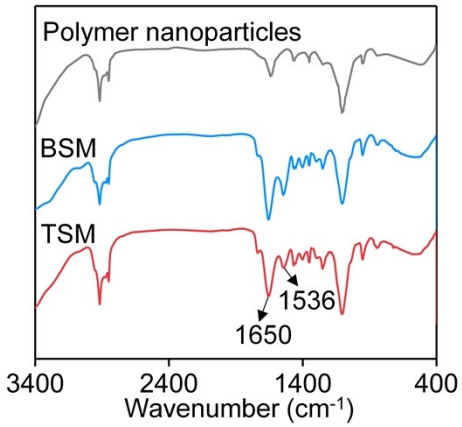

Fig. S2. FTIR spectra of polymer nanoparticles, BSM and TSM.

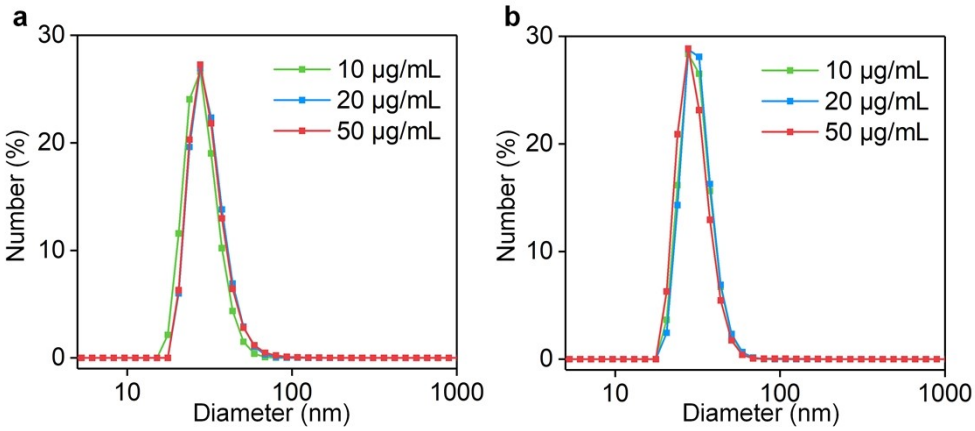

Fig. S3. Hydrodynamic diameter profiles of (a) BSM and (b) TSM at the different concentrations of 10, 20 and 50 μg/mL.

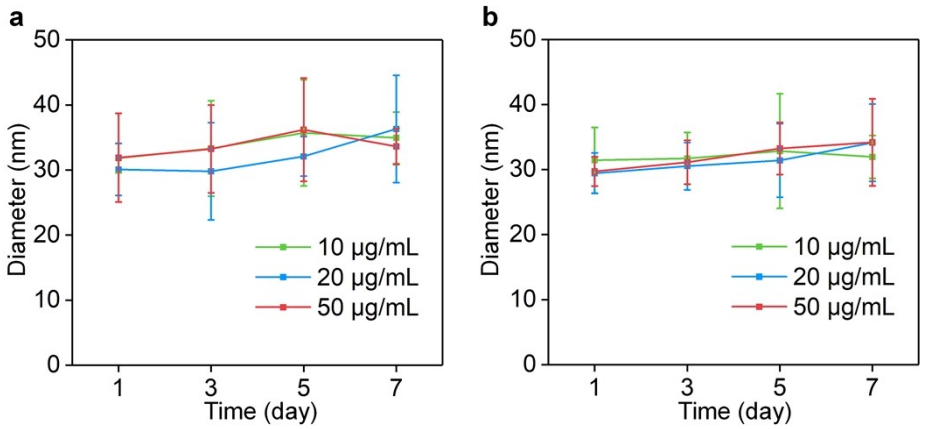

Fig. S4. Hydrodynamic diameters of (a) BSM and (b) TSM at the different concentrations after storage for 1, 3, 5 and 7 days.

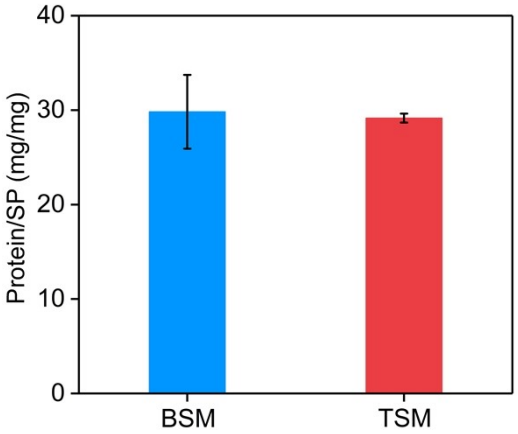

Fig. S5. Amount of protein on surface of nanoparticles measured via BCA protein quantification analysis.

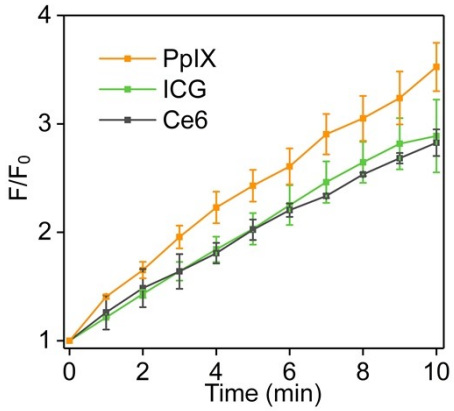

Fig. S6. The $^1O_2$ generation evaluation for SOSG solutions containing PpIX, ICG and Ce6 after 808 nm laser irradiation by measuring the fluorescence enhancement (F/F_0).

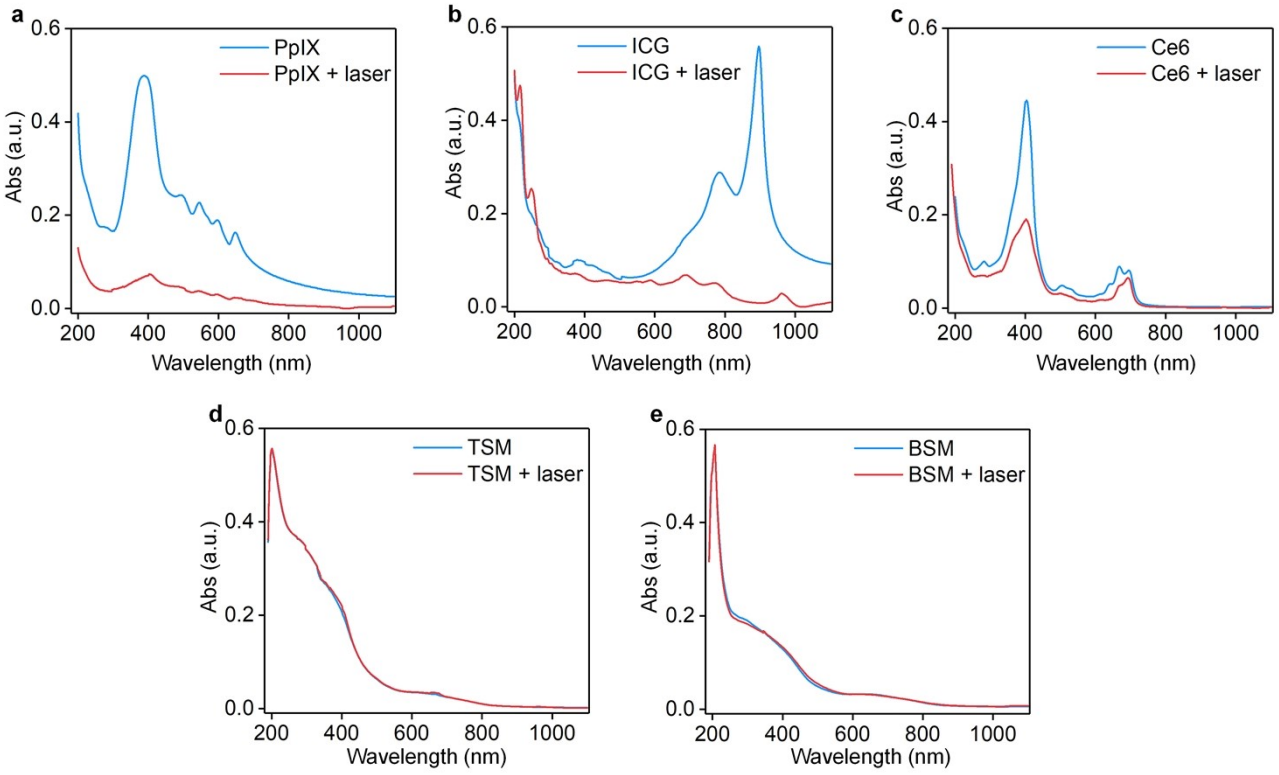

Fig. S7. The UV-vis absorbance spectra of (a) PpIX, (b) ICG, (c) Ce6, (d) TSM and (e) BSM before and after laser irradiation for 10 min.

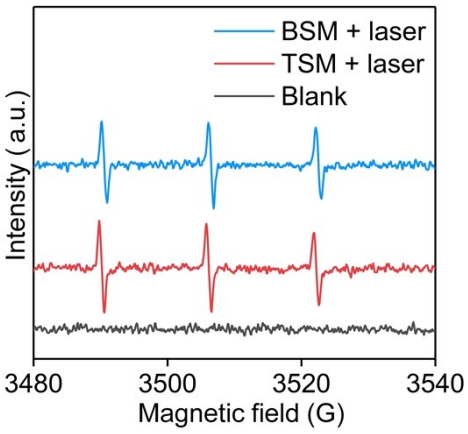

Fig. S8. ESR spectra of the generated $^1O_2$ for blank, BSM and TSM after laser irradiation.

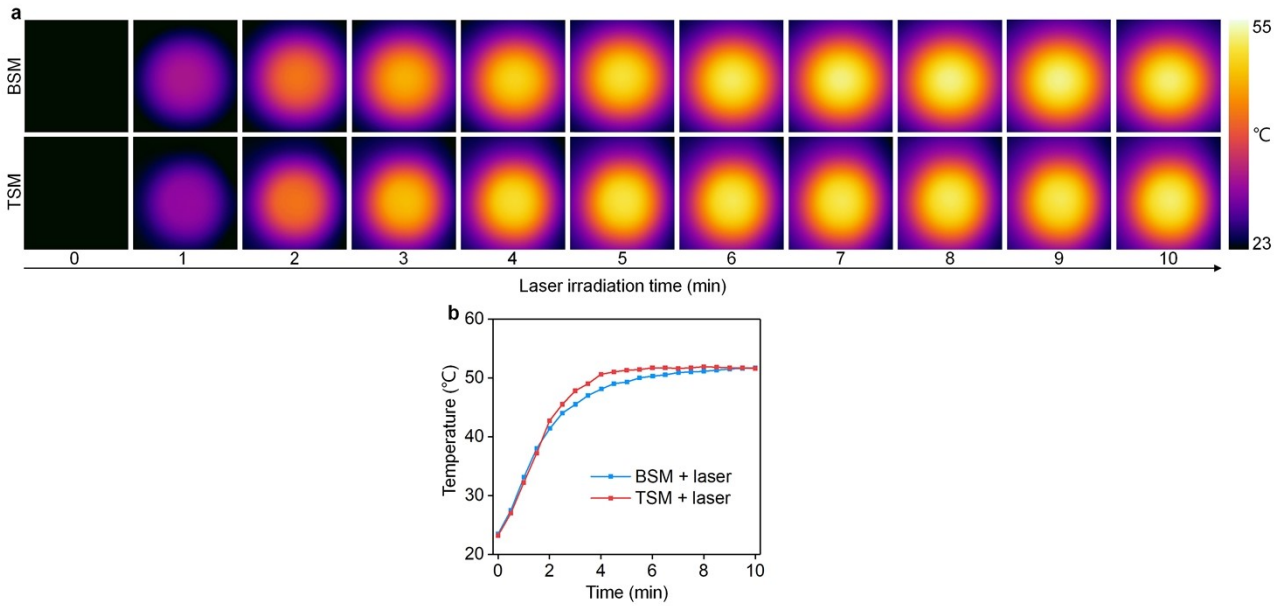

Fig. S9. (a) Thermal images of solutions containing BSM and TSM under 808 nm laser irradiation for different times. (b) Temperatures of solutions containing BSM and TSM under laser irradiation.

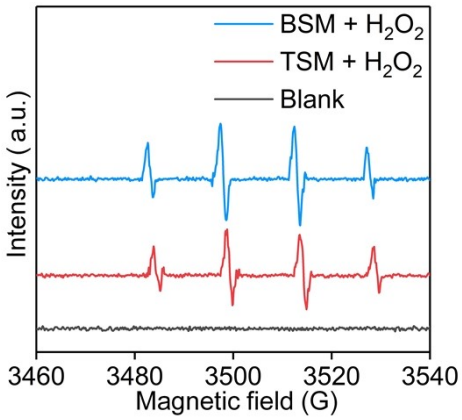

Fig. S10. ESR spectra of the generated ·OH for blank, BSM and TSM after incubation with H_2O_2 and GSH.

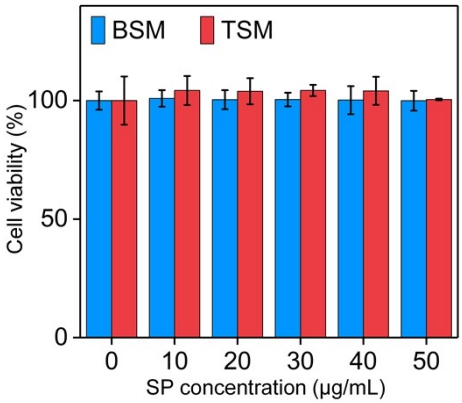

Fig. S11. Cell viability analysis of BSM- and TSM-treated 4T1 cells at different SP concentrations for 24 h (n = 5).

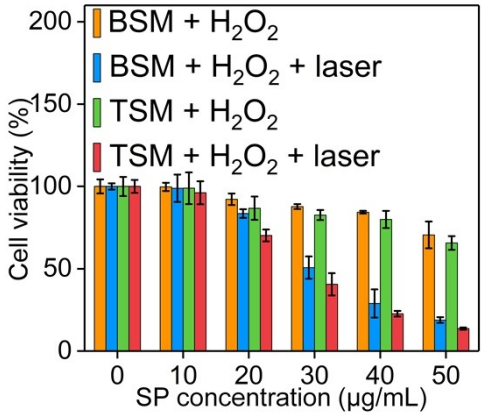

Fig. S12. Cell viability analysis of BSM- and TSM-treated 4T1 cells at various SP concentrations (n = 5) in the presence of H_2O_2 without or with 808 nm laser irradiation (1 W/cm^2, 5 min).

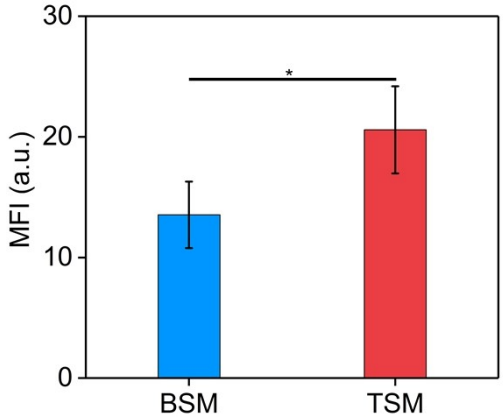

Fig. S13. Mean fluorescence intensity of BSM- and TSM-treated 4T1 cells (n = 3).

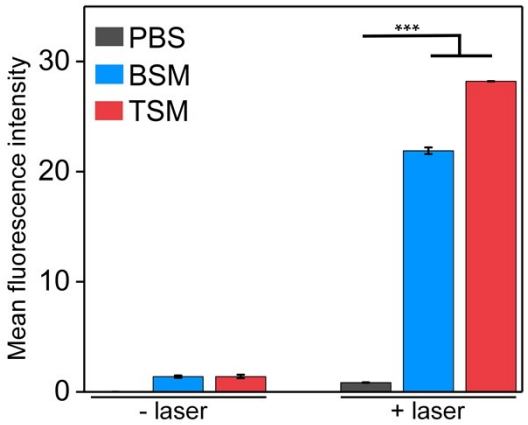

Fig. S14. Mean fluorescence intensity of ROS signals inside 4T1 cells after different treatments to evaluate the intracellular ROS generation (n = 3).

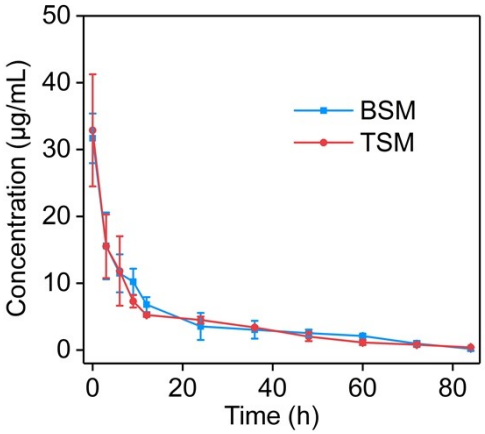

Fig. S15. Pharmacokinetic analysis of BSM and TSM after intravenous injection to tumor-bearing mice.

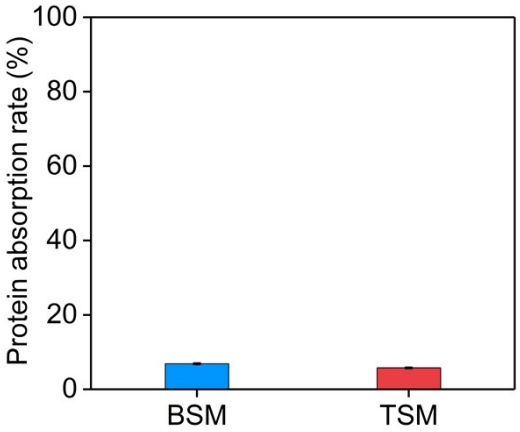

Fig. S16. Protein absorption analysis for BSM and TSM after incubation with BSA.

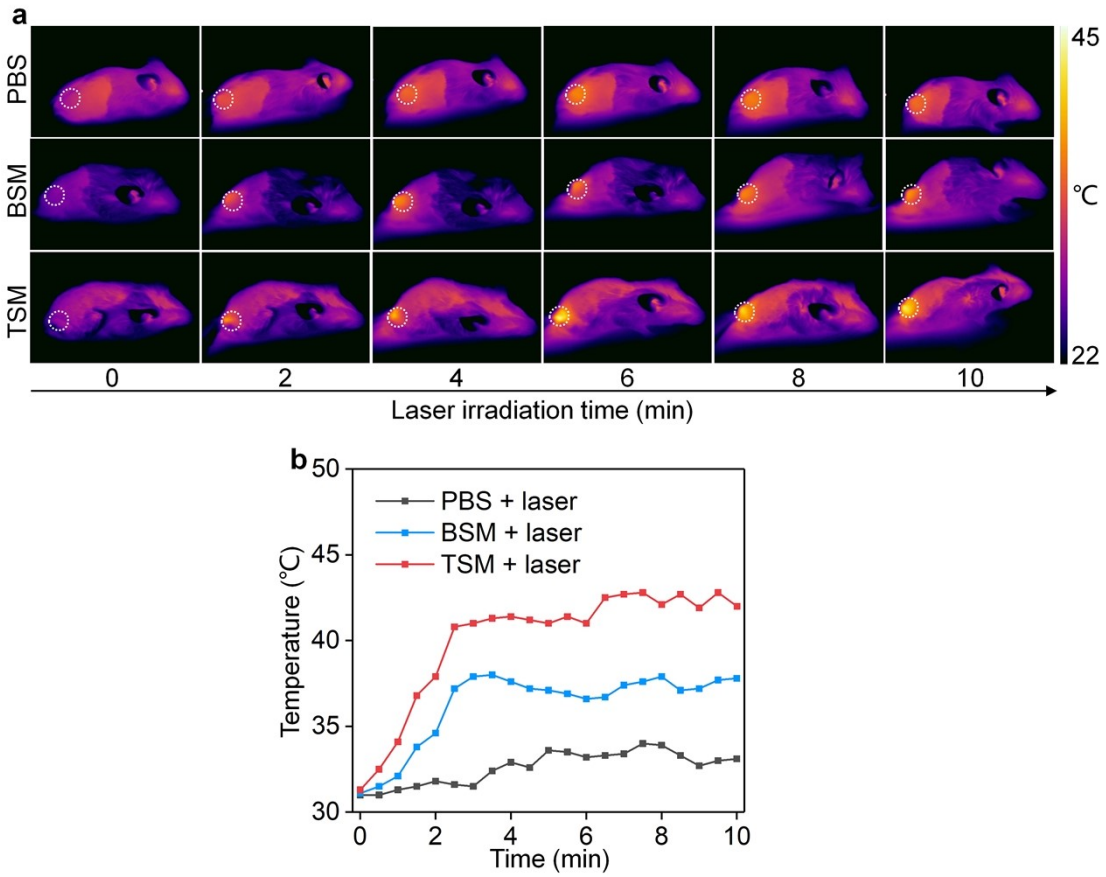

Fig. S17. (a) Thermal images of tumor-bearing mice after intravenous injection of PBS, BSM and TSM with laser irradiation for different time. (b) Temperatures of tumors under laser irradiation.

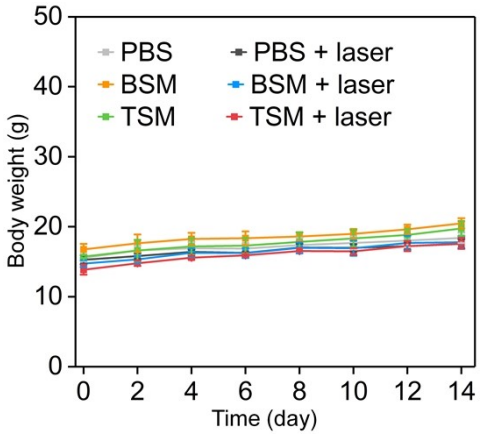

Fig. S18. Body weights of 4T1 tumor-bearing mice after intravenous injection of PBS, BSM and TSM with or without laser irradiation from 0 to 14 days (n = 4).

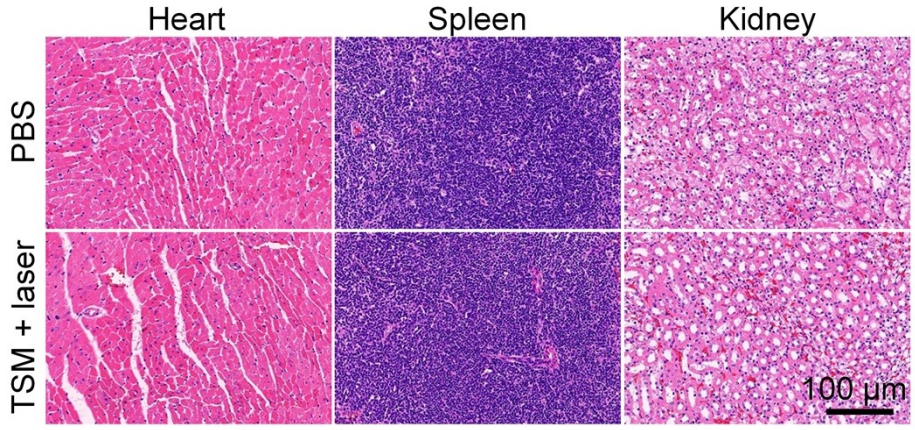

Fig. S19. Representative H&E staining images of heart, spleen, and kidney of mice in PBS control and TSM + laser groups.

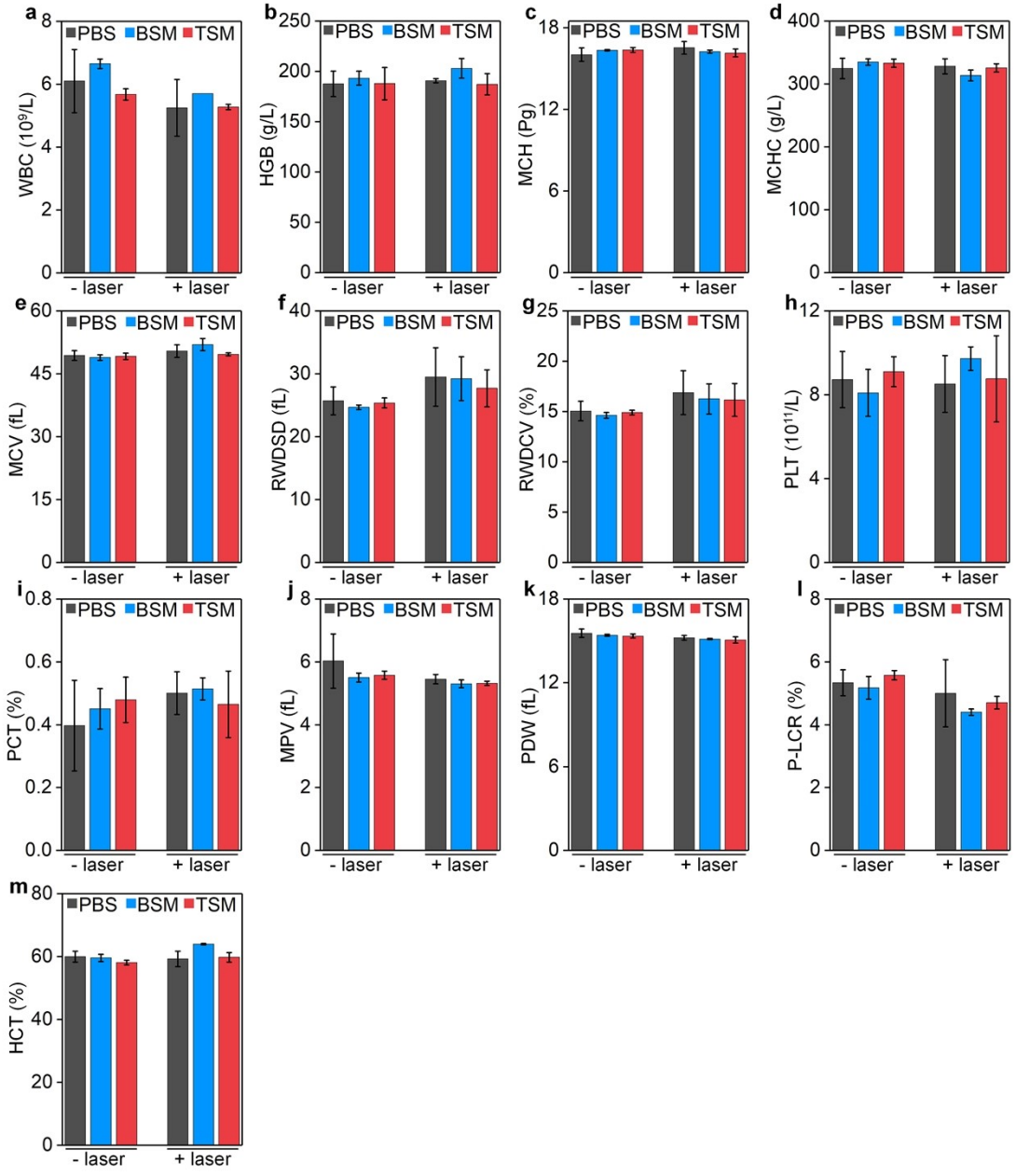

Fig. S20. The levels of (a) WBC, (b) HGB, (c) MCH, (d) MCHC, (e) MCV, (f) RWDSD, (g) RWDCV, (h) PLT,

(i) PCT, (j) MPV, (k) PDW, (l) P-LCR, and (m) HCT in blood samples of mice.

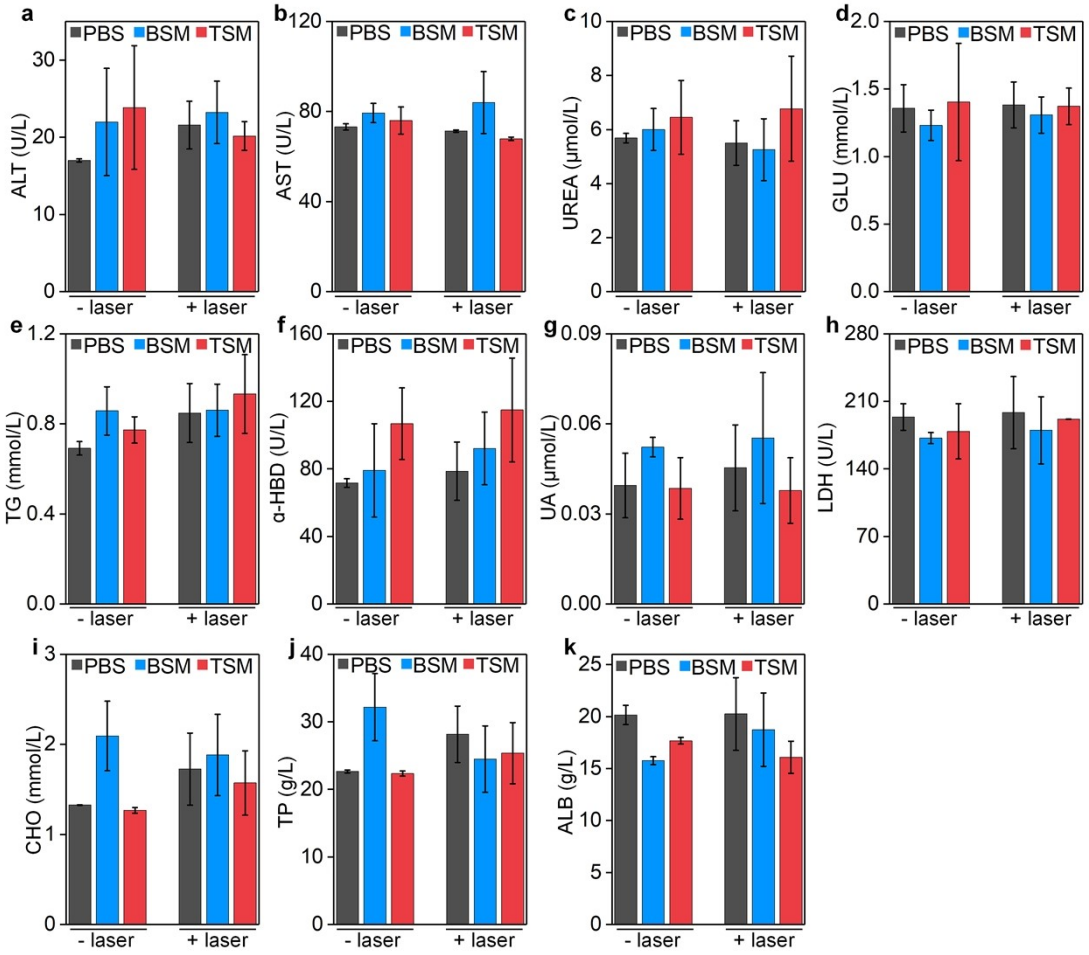

Fig. S21. The levels of (a) ALT, (b) AST, (c) UREA, (d) GLU, (e) TG, (f) α-HBD, (g) UA, (h) LDH, (i) CHO, (j) TP and (k) ALB in blood samples of mice.